SCIENCE CHINA
Technological Sciences

• Article •

December 2014 Vol.57 No.12: 2328–2334
doi: 10.1007/s11431-014-5647-5

A general, rapid and solvent-free approach to fabricating nanostructured polymer surfaces

TIAN Wei[1*], HUANG LongBiao[2], WANG DaWei[3] & Roy V. A. L.[2*]

[1] *Key Laboratory of Space Applied Physics and Chemistry, Ministry of Education and Shaanxi Key Laboratory of Macromolecular Science and Technology, School of Science, Northwestern Polytechnical University, Xi'an 710072, China;*
[2] *Center of Super-Diamond and Advanced Films (COSDAF), and Department of Physics and Materials Science, City University of Hong Kong, Hong Kong, China;*
[3] *School of Chemistry and Chemical Engineering, and Lehn Institute of Functional Materials, Sun Yat-Sen University, Guangzhou 510275, China*

Received March 9, 2014; accepted May 31, 2014; published online September 2, 2014

A general, rapid and solvent-free approach is proposed to fabricate nanostructured polymer surfaces by coupling ultrasonic vibration and anodized aluminum oxide templating. With our approach, hollow nanorods or nanofibers with controlled diameter and length are prepared on polymer surfaces. The whole fabrication process is completed in ~30 s and equally applicable to polymers of different crystalline structures. The wettability of the as-fabricated polymer surfaces (being hydrophilic, hydrophobic, highly hydrophobic or even superhydrophobic) is readily regulated by adjusting the welding time from 0 s to a maximum of 10 s. Our approach can be a promising industrial basis for manufacturing functional nanomaterials in the fields of electronics, optics, sensors, biology, medicine, coating, or fluidic technologies.

nanomaterials, nanostructured polymer surfaces, ultrasonic vibration, anodized aluminum oxide template, wettability

Citation: Tian W, Huang L B, Wang D W, et al. A general, rapid and solvent-free approach to fabricating nanostructured polymer surfaces. Sci China Tech Sci, 2014, 57: 2328–2334, doi: 10.1007/s11431-014-5647-5

1 Introduction

Polymers with regularly nanostructured surface have attracted extensive attentions due to their various nanopatterned morphologies and tunable wettablity, leading to potential applications in superhydrophobic surfaces [1,2], optoelectronic devices [3], bio-related and medicinal industries [4]. Typical approaches employed for fabricating nanostructured polymer surfaces can be classified into "bottom-up" and "top-down" strategies [5]. In bottom-up approaches, the key point is to select suitable solvents to dissolve polymer samples [6,7], which, however, can be difficult for complex conjugated polymers and crystalline polymers with high melting point (T_m). Even if involatile solvents can be found and used, they may remain as impurities on polymer surfaces, since they can hardly be totally evaporated. Among top-down approaches, anodized aluminum oxide (AAO) templating strategies [2,8,9] show advantages over other ones (including radiation techniques [10], prepatterned template approach [11] and direct writing [12]), with which nanostructured polymer surfaces are fabricated by simply wetting polymer melts or solutions into the nanopores of AAO. The drawback of this strategy is that it requires long processing time (hours to days) [13–15] or —— similar to the case in bottom-up approaches —— involatile solvents for complex conjugated polymers and crystalline polymers with high T_m [16].

*Corresponding authors (email: happytw_3000@163.com; val.roy@cityu.edu.hk)

In our previous work, tepee-like bundles as micro/nanostructures were fabricated on the surfaces of polystyrene by AAO templating [17]. Here, we propose a rapid and solvent-free approach to fabricating nanostructured surfaces of polymers of various crystalline structures. By coupling ultrasonic vibration with AAO templating, polymers are melted rapidly and then wet and cover the walls of AAO channels. In this way, hollow nanorods or nanofibers with controlled diameter and length are fabricated on polymer surfaces. The whole process is completed in ~30 s and equally applicable to polymers of different crystalline structures (with T_m, or glass transition temperature, T_g, from 80 to 300°C), and does not involve any solvent. Moreover, by adjusting the welding time, the wettability of nanostructured polymer surfaces can be readily regulated (from hydrophilic to hydrophobic to highly hydrophobic and even to superhydrobic). The approach we describe in this paper can be extended to fabricating the surfaces of metals with low melting point (for example, aluminum [18]) and can be a promising industrial basis for manufacturing functional nanomaterials in the fields of electronics, optics, sensors, biology, medicine, coating, or fluidic technologies [19–21].

2 Experiment procedure

Materials. Amorphous polymers, semi-crystalline polymers, and highly crystalline polymers were used in this study. These polymer plates included polystyrene (PS, T_g= 150°C), poly(methyl methacrylate) (PMMA, T_g=105°C), polycarbonate (PC, T_g=150°C), polyethylene (PE, T_m= 129°C), polypropylene (PP, T_m=150°C), poly(ethylene terephthalate) (PET, T_m=129°C) and poly(3-hexylthiophene) (P3HT, T_m =238°C). The polymers were cut into rectangular plates with dimensions of 25 mm × 20 mm × 1.5 mm before used. AAO templates were purchased from Whatman Co Ltd. (U.K.) with through-hole channel diameter of 200 nm or 100 nm and channel length of about 60 μm. Other chemical reagents including NaOH, ethanol and deionized water were purchased from Alfa Aesar China Co. Ltd.

Fabrication of nanostructred polymer surfaces. The ultrasonic welding system, processing principle and fabrication process were described in detail and discussed in supporting information (SI).

Characterization. The nanostructured polymer surfaces were characterized using scanning electron microscopy (SEM, JEOL Model JSM-6490). Before characterization, the surface of samples was coated with Au film (5.0 nm in thickness). The static water contact angle (CA, θ) measurements were carried out using a Rame-hart Model 250-F1 Standard Goniometer with DROP Image Advanced 2.1 at ambient temperature. A drop of ion-exchanged water (3 μL for static water CA measurements) was placed on the as-fabricated polymer surface using microsyringe appurtenance, then a photograph was taken. CA was determined by fitting a Young-Laplace curve around the drop. Five parallel measurements were conducted for each sample, and the average contact angle value was used as the result for each sample.

3 Results and discussion

Our experiments were based on polymers of different crystalline structures, including amorphous polymers (PC, PS and PMMA), semi-crystalline polymers (PE and PP) and highly crystalline polymers (PET and P3HT). In a typical procedure (Figure 1, and see Figure S1, Section 1 and 2 in SI for details), two polymer plates of the same material with crossed welding lines on their surfaces were brought to contact[1)]. Friction between the polymer plates were induced by ultrasonic vibration to generate enough heat for melting polymer plates and enabling the molten polymer to flow into the channels (180±20 or 265±24 nm in diameter, 60 μm in length; see the SEM images in Figure S2 in SI) of AAO templates. This molten polymer solidified quickly (~10 s) after terminating ultrasonic vibration. To remove the AAO template, the polymer/AAO template was immersed in a 5 wt.% NaOH solution and washed with deionized water and ethanol. Prior to characterization with SEM, the polymer was dried under vacuum at room temperature for 5 h.

The key feature of this approach is that it is equally applicable to polymers with quite different crystalline/chemical structures and/or physicochemical properties. By ultrasonic vibration, sufficient frictional heat is generated within seconds (≤10 s) such that all the polymers used in our experiments can be melted. The adhesive forces between polymer melts and the walls of AAO channels are much stronger than the cohesive forces of polymer melts; consequently, polymer melts wet and cover the walls of AAO channels, leading to the growth of nanosized, hollow polymer fibers (cf. Figure 2 for the SEM images of PC, PS, PMMA, PE, PP, PET and P3HT) [8]. Due to the intrinsic van der Waals interaction and the hydrostatic dilation stress during the removing of ethanol [22–24], these fibers come into contact with adjacent ones and form discrete fiber bundles while spreading over the polymer surface. As expected, the average diameters of individual fibers are close to the average diameters of AAO channels (cf. Table 1), suggesting that the dimension of fibers and consequently, the surface structure of polymers, can be tuned via AAO template. In fact, the average diameter of hollow fibers decreased to

1) Herein, two polymers plates were used to prevent heat loss during friction. One polymer plate was attached to the horn, and the other one was fixed on the ceramic chap placed between AAO template and the pedestal. Crossed welding lines were made on the surfaces of two polymers prior to friction, since these crossed welding lines were essential for rapidly generating a large amount of friction heat.

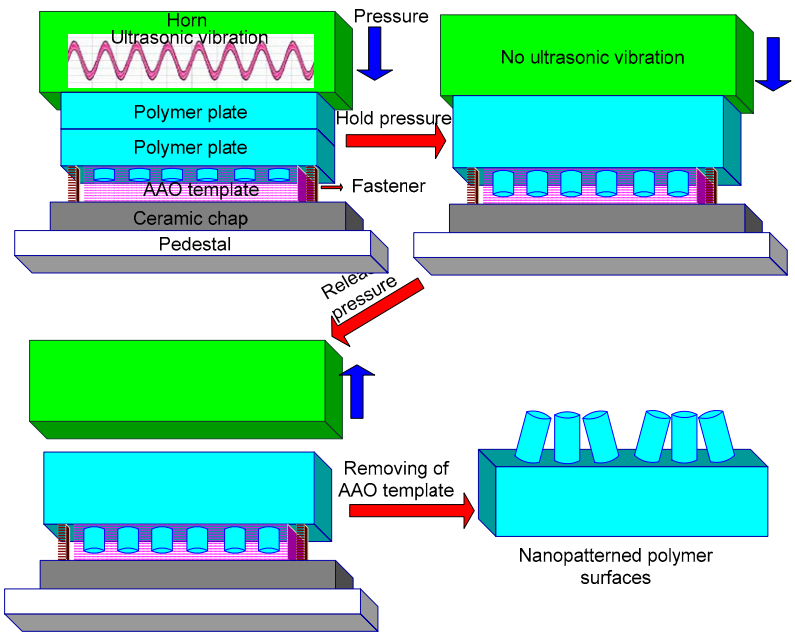

Figure 1 Fabrication process of nanostructured polymer surfaces.

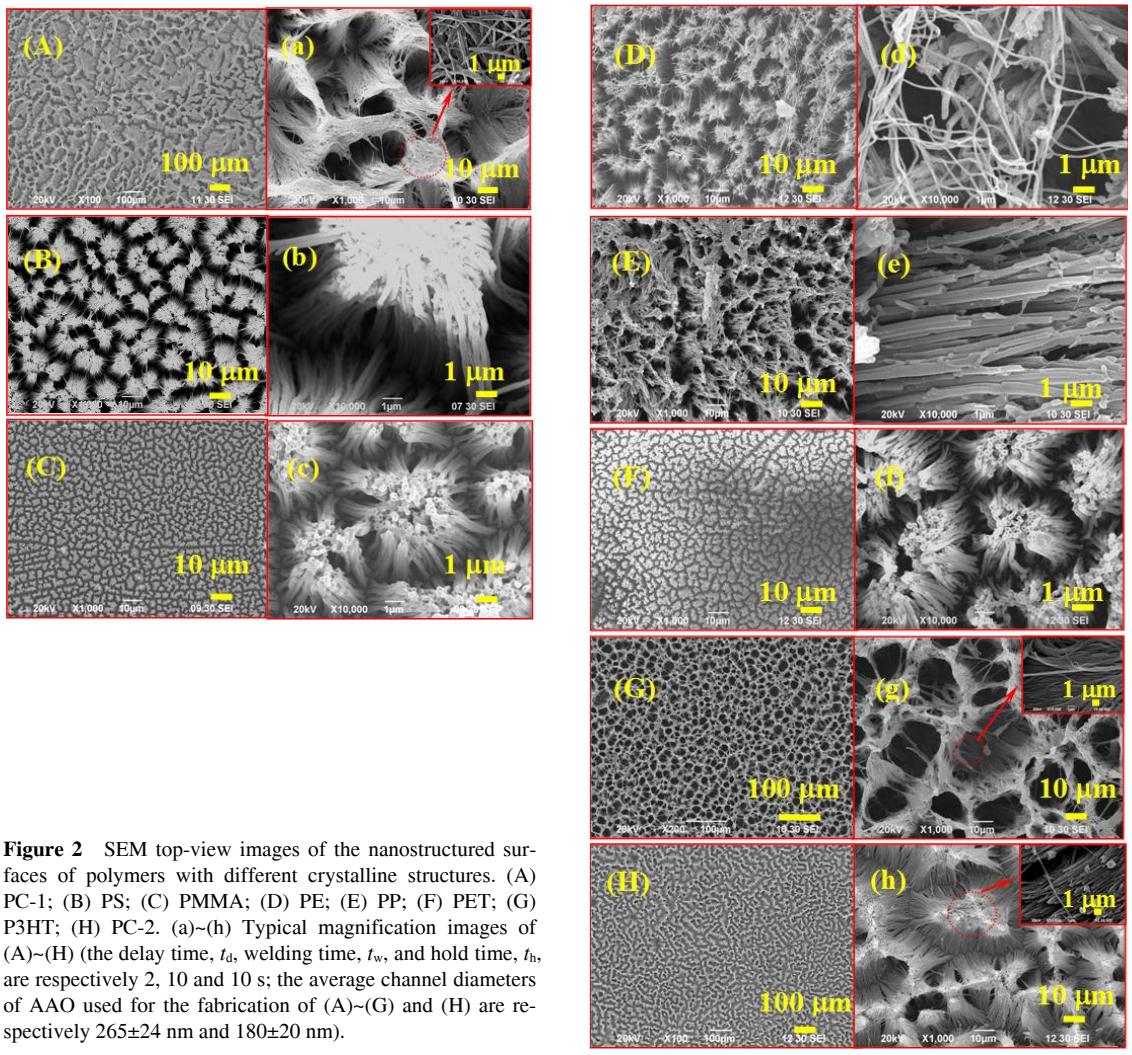

Figure 2 SEM top-view images of the nanostructured surfaces of polymers with different crystalline structures. (A) PC-1; (B) PS; (C) PMMA; (D) PE; (E) PP; (F) PET; (G) P3HT; (H) PC-2. (a)~(h) Typical magnification images of (A)~(H) (the delay time, t_d, welding time, t_w, and hold time, t_h, are respectively 2, 10 and 10 s; the average channel diameters of AAO used for the fabrication of (A)~(G) and (H) are respectively 265±24 nm and 180±20 nm).

Table 1 Average diameter of fibers on nanostructured polymer surfaces in Figure 1

Samples	Diameter (nm)
PC-1[a)]	256±36
PS[a)]	278±24
PMMA[a)]	259±18
PE[a)]	278±15
PP[a)]	269±11
PET[a)]	245±16
P3HT[a)]	249±28
PC-2[b)]	195±17

a) AAO templates with average channel diameter of 265±24 nm were used in the fabrication process; b) AAO templates with average channel diameter of 180±20 nm were used in the fabrication process

~195±17 nm when AAO template with smaller channels (~180±20 nm on average) was used in our experiments (cf. Figure 2(H)).

While universal, our approach is quite rapid and solvent-free. Benefiting from ultrasonic vibration, the involvement of involatile solvent and the preheat of AAO template and/or polymer were avoided in our approach, which is advantageous over ultrasonic vibration-assisted hot embossing or nanoimprint lithography approach [25–28]. Additionally, the heat induced by ultrasonic vibration completely dissipated within several seconds after the vibration was terminated. Therefore, the whole processing cycle, which includes a delay time (t_d=2 s), a welding time (t_w≤10 s, cf. Figures 2 and 3) and a hold time (t_h =10 s), can be limited into around half a minute, whereas the cycle may last several minutes to a few hours or days in traditional melt wetting process [13–15]. Our approach is particularly advantageous to PET and P3HT —— the surfaces of these highly crystalline/conjugated polymers are usually difficult to be treated, due to their high T_m and special crystalline structures [29,30].

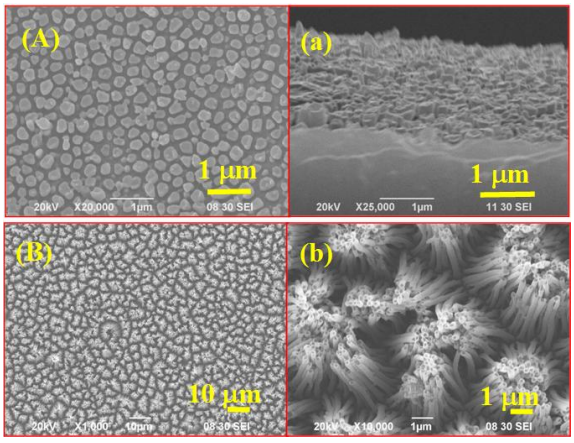

Figure 3 (Color online) SEM top-view ((A), (B), and (b)) and cross-section (a) images of nanostructured PC surfaces. (A) and (a) t_w=2 s; (B) t_w=5 s; (b) typical magnification image of (B) (t_d and t_h are 2 s and 10 s, respectively; channel diameter: 265±24 nm).

The key parameter of controlling the length of fibers as well as the morphology of polymer surface is the welding time. When t_w is short, insufficient heat is generated and only allows limited molten polymers to cover the AAO channel walls before the polymers solidify. Therefore, short, discrete hollow nanorods (200–300 nm in height) formed on polymer surfaces (Figure 3(A), t_w=2 s for PC). Conversely, long t_w enables much more molten polymers to cover the AAO channel walls to form bundles of short hollow fibers (Figure 3(B), t_w=5 s for PC). Further increase in t_w leads to formation of bundles of long hollow fibers, which are readily to bend (Figure 2(A), t_w=10 s for PC). Although the lengths of fibers vary significantly with t_w, the diameters are —— as expected —— still well controlled, comparable to that of AAO channels.

We emphasize that t_w may vary from polymer to polymer, or be the same for several different polymers. Likely, the chemical structures of polymers play an important role in t_w. For various main chains and functional groups in polymer structures, the responsive abilities to ultrasonic vibration can be totally different [25], the total heat generated in the whole polymer, however, can be different or quite close. Consequently, t_w=5 s was sufficient for PC to form bundles of short fibers (Figure 3(B)), while t_w had to be 10 s for PS, PMMA and PET to form similar structures (Figures 2(B), (C) and (F)) or PC-1, PE, PP and P3HT to form bundles of long fibers (Figures 2(A), (D), (E) and (G)).

Once nanosized fibers/rods are fabricated, the surface properties (for instance, wettability, photoelectric properties, and thermal conductivity) generally change dramatically. In this context, our approach can be used to readily tune the surface properties of polymers. Here, we demonstrate how to regulate the wettability of polymer surface, evaluated by the static water contact angle, by simply adjusting t_w. As shown in Figure 4(a) (the insets are the optical images of a water droplet on the respective surfaces), the pristine PC surface is hydrophilic (t_w=0, θ=75°) while the nanostructured PC surface can be hydrophobic (t_w=2 s, θ=101°), highly hydrophobic (t_w=5 s, θ=135°) or superhydrophobic (t_w=10 s, θ=155°). The only parameter used for adjusting the wettability/CA is t_w. The wettability/CA of all the other polymers in our experiments shows similar trends, except that nanostructured PMMA and PP surface are highly hydrophobic other than superhydrophobic (Figure 4(b)). The underlying physical chemistry of wettability regulation may be attributed to the roughness of nanostructured polymer surface [31]. Briefly, the length of polymer fibers increases with t_w, which results in increased surface roughness and in turn enables polymer surfaces to provide more air pockets between polymer fibers and to maintain the Cassie-Baxter state [32]; consequently, the nanostructured polymer surfaces show improved hydrophobicity. Similar results were obtained in our previous work (on the patterned surfaces of PS) [17].

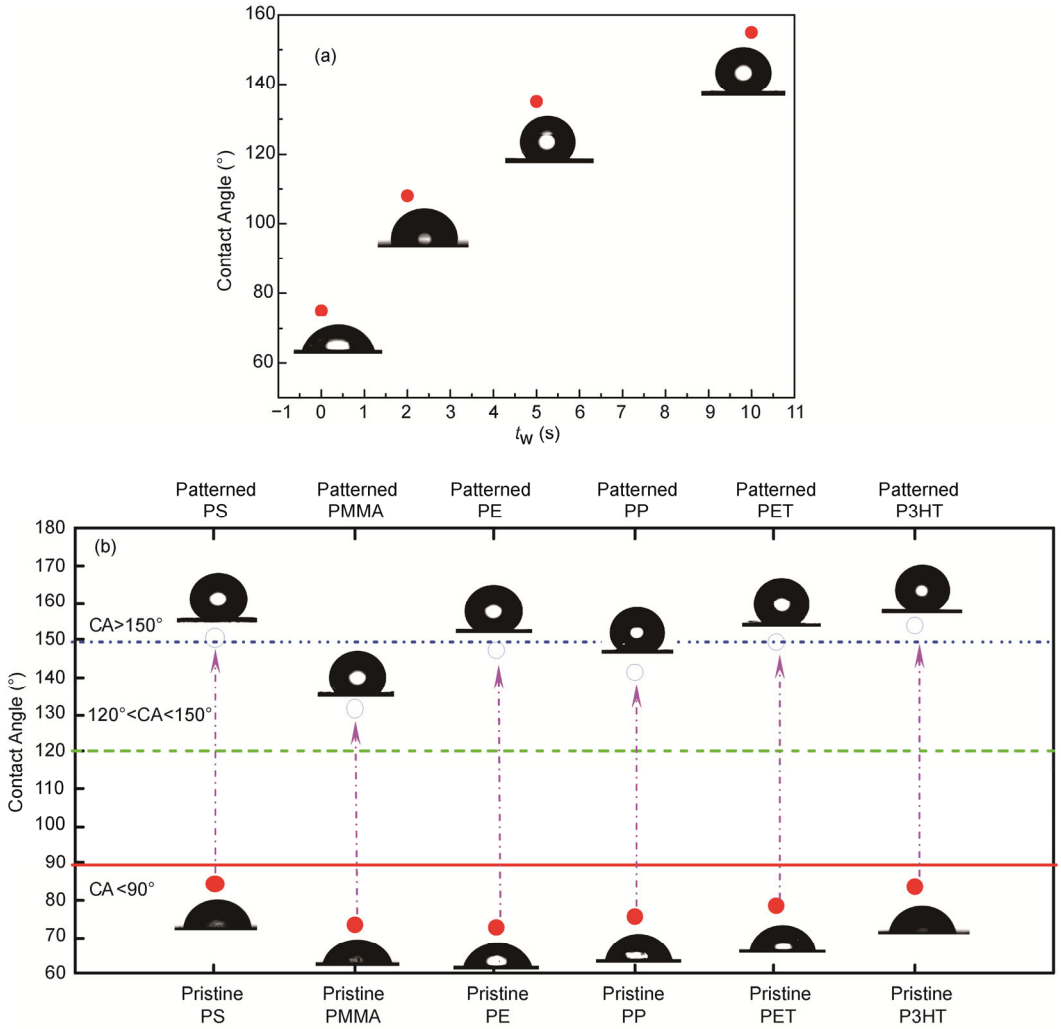

Figure 4 (Color online) Static water CAs of nanostructured polymer surfaces. (a) Dependence of the CAs of PC surfaces on t_w; (b) CAs of the pristine polymer surfaces and the coresponding nanostructured polymer surfaces shown in Figure 2. The inserts in (a) and (b) are the optical images of a water droplet on the respective polymer surface.

4 Conclusion

In conclusion, we demonstrate that the combination of ultrasonic vibration and AAO templating strategy can be used to rapidly fabircate nanosized, hollow rods or fibers on the surfaces of various polymers. The key parameter of our approach is the welding time, which can be used to regulate the length of polymer rods/fibers and the wettability of nanostructured polymer surfaces. Of particular interests in the future research is to regulate the optoelectronical property of conjugated polymer (such as P3HT [33]) with our approach, which should be of significant importance for the fabrication of polymer-based optoelectronic devices [34,35].

This work was supported by the National Natural Science Foundation of China (Grant No. 21374088). W.T. thanks the grant from the Program for New Century Excellent Talents of Ministry of Education (Grant No. NCET-13-0476), the Program of Youth Science and Technology Nova of Shaanxi Province of China (Grant No. 2013KJXX-21), and the Program of New Staff and Research Area Project of NPU (Grant No. 13GH014602).

1 Lee W, Jin M K, Yoo W C, et al. Nanostructuring of a polymeric substrate with well-defined nanometer-scale topography and tailored surface wettability. Langmuir, 2004, 20: 7665–7669
2 Lee Y W, Park S H, Kim K B, et al. Fabrication of hierarchical structures on a polymer surface to mimic natural superhydrophobic surfaces. Adv Mater, 2007, 19: 2330–2335
3 Xu Y Y, Zhang F, Feng X L. Patterning of conjugated polymers for organic optoelectronic devices. Small, 2011, 7: 1338–1360
4 Guo Z G, Liu W M, Su B L. Superhydrophobic surfaces: From natural to biomimetic to functional. J Colloid Inter Sci, 2011, 353: 335–355
5 Del Campo A, Arzt E. Fabrication approaches for generating complex micro- and nanopatterns on polymeric surfaces. Chem Rev, 2008, 108: 911–945
6 Widawski G, Rawiso M, Francois B. Self-organized honeycomb morphology of star-polymer polystyrene films. Nature, 1994, 369: 387–389
7 Zhang J, Yu X, Yang P, et al. Microphase separation of block copolymer thin films. Macromol Rapid Commun, 2010, 31: 591–608

8 Steinhart M, Wendorff J H, Greiner A, et al. Polymer nanotubes by wetting of ordered porous templates. Science, 2002, 296: 1997
9 Zhu S J, Li Y F, Zhang J H, et al. Biomimetic polyimide nanotube arrays with slippery or sticky superhydrophobicity. J Colloid Interface Sci, 2010, 344: 541–546
10 Ito H. Chemical amplification resists for microlithography. Adv Polym Sci, 2005, 172: 37–245
11 Krebs F C. Fabrication and processing of polymer solar cells: A review of printing and coating techniques. Sol Energy Mater Sol Cells, 2009, 93: 394–412
12 Zhang Y L, Chen Q D, Xia H, et al. Designable 3D nanofabrication by femtosecond laser direct writing. Nano Today, 2010, 5: 435–448
13 Steinhart M, Wendorff J H, Wehrspohn R B. Nanotubes à la carte: Wetting of porous templates. ChemPhysChem, 2003, 4: 1171–1176
14 Sun Y M, Steinhart M, Zschech D, et al. Diameter-dependence of the morphology of PS-b-PMMA nanorods confined within ordered porous alumina templates. Macromol Rapid Commun, 2005, 26: 369–375
15 Zhang M F, Dobriyal P, Chen J T, et al. Wetting transition in cylindrical alumina nanopores with polymer melts. Nano Lett, 2006, 6: 1075–1079
16 Cannon J P, Beardena S D, Goldb S A. Effect of wetting solvent on poly(3-hexylthiophene) (P3HT) nanotubles fabricated via template wetting. Synth Met, 2010, 160: 2623–2627
17 Tian W, Yung K L, Xu Y, et al. Beta-cyclodextrin and its hyperbranched polymers-induced micro/nanopatterns and tunable wettability on polymer surfaces. Nanoscale, 2011, 3: 5147–5155
18 Belova V, Gorin D A, Shchukin D G, et al. Selective ultrasonic cavitation on patterned hydrophobic surfaces. Angew Chem Int Ed, 2010, 49: 7129–7133
19 Cao B Y, Li Y W, Kong J, et al. High thermal conductivity of polyethylene nanowire arrays fabricated by an improved nanoporous template wetting technique. Polymer, 2011, 52: 1711–1715
20 Tao L S, Desai T A. Aligned arrays of biodegradable poly(ε-caprolactone) nanowires and nanofibers by template synthesis. Nano Lett, 2007, 7: 1463-1468
21 Yun H, Kim W S, Kim K H, et al. Highly enhanced interfacial adhesion properties of steel-polymer composites by dot-shaped surface patterning. J Appl Phys, 2011, 109: 074302
22 Girifalco L A, Hodak M, Lee R S. Carbon nanotubes, buckyballs, ropes, and a universal graphitic potential. Phys Rev B, 2000, 62: 13104
23 Li J, Cassell A, Delzeit L, et al. Novel three-dimensional electrodes: Electrochemical properties of carbon nanotube ensembles. J Phys Chem B, 2002, 106: 9299–9305
24 Liu H, Li S H, Zhai J, et al. Self-assembly of large-scale micropatterns on aligned carbon nanotube films. Angew Chem Int Ed, 2004, 43: 1146–1149
25 Liu S J, Dung Y T. Hot embossing precise structure onto plastic plates by ultrasonic vibration. Polym Eng Sci, 2005, 45: 915–925
26 Mekaru H, Nakamura O, Maruyama O, et al. Development of precision transfer technology of atmospheric hot embossing by ultrasonic vibration. Microsyst Tech, 2007, 13: 385–391
27 Lin C H, Chen R S. Ultrasonic nanoimprint lithography: A new approach to nanopatterning. J Microlith Microfab Microsyst, 2006, 5: 011003
28 Lee C H, Jung P G, Lee S M, et al. Replication of polyethylene nano-micro hierarchical structures using ultrasonic forming. J Micromech Microeng, 2010, 20: 035018
29 Li S C, Lu L N. Melt rheological properties of reactive compatibilized HDPE/PET blends. J Appl Polym Sci, 2008, 108: 3559–3564
30 Wu Z, Petzold A, Henze T, et al. Temperature and molecular weight dependent hierarchical equilibrium structures in semiconducting poly(3-hexylthiophene). Macromolecules, 2010, 43: 4646–4653
31 Lee D J, Kim H M, Song Y S, et al. Water droplet bouncing and superhydrophobicity induced by multiscale hierarchical nanostructure. ACS Nano, 2012, 6: 7656–7664
32 Marmur A. Wetting on hydrophobic rough surfaces: To be heterogeneous or not to be? Langmuir, 2003, 19: 8343–8348
33 Baek S J, Park J B, Lee W J, et al. A facile method to prepare regioregular poly(3-hexylthiophene) nanorod arrays using anodic aluminium oxide templates and capillary force. New J Chem, 2009, 33: 986–990
34 Byun J, Kim Y, Jeon G, et al. Ultrahigh density array of free-standing poly(3-hexylthiophene) nanotubes on conducting substrates via solution wetting. Macromolecules, 2011, 44: 8558–8562
35 Wang J H, Min G Q, Song Z T, et al. Solvent-infiltration imprint lithography: A novel method to prepare large area poly(3-hexylthiophene) micro/nano-patterns. J Mater Chem, 2012, 22: 21154–21158

Supporting information: Experimental

1 Ultrasonic welding system

A commercial ultrasonic welding apparatus was purchased from Dongguan Shek Pai Nekon Ultrasonic Machinery Co., LTD (China), with generator frequency of 35 kHz, power of 500 W and maximum amplitude of 35 μm (Figure S1). The apparatus consisted of a control part (Figure S1-1), a functional part (Figure S1-2) and a leveling anvil (Figure S1-4). As the core component of functional part, the resonance stack (Figure S1-3) comprised of a piezoelectric ultrasonic converter (Figure S1-3-1) which converted electrical signal into mechanical oscillation, a so-called 'booster' (Figure S1-3-2) for amplitude transformation and a horn (Figure S1-3-3) for transmitting the vibration to polymer specimens [S1]. During embossing, the horn's bottom contacted with the polymer plate. When the piezoelectric device started vibrating, the horn transferred and enlarged the amplitude of the waves and generated frictional heat, which enabled the polymer to be heated to its T_g or T_m under a given pressure (45 Pa in our experiments). Subsequently, the polymer melt wetted and covered the channel walls in mold [S2].

2 Procedure of nanopatterning polymer surfaces (cf. Scheme 1)

(1) One polymer plate was attached to the horn and another one was fixed on the ceramic chap placed between AAO template and the pedestal to prevent heat loss. It should be pointed out that crossed welding lines were made on the surfaces of two polymers prior to friction, since these crossed welding lines were essential for rapidly generating a large amount of friction heat. After the mold contacted with two polymer plates, the pressing force was gradually increased up to 45 Pa and was maintained during a delay time (t_d=2 s). During the welding time (t_w=2, 5 or 10 s), friction heat was generated between the two polymer plates and the